η^1-Arene Complexes as Intermediates in the Preparation of Molecular Phosphorescent Iridium(III) Complexes

Miguel A. Esteruelas,*[a] Daniel Gómez-Bautista,[a] Ana M. López,[a] Enrique Oñate,[a] Jui-Yi Tsai,[b] and Chuanjun Xia[b]

Abstract: Molecular phosphorescent heteroleptic bis-tridentate iridium(III) emitters have been prepared via η^1-arene intermediates. In the presence of 4.0 mol of AgOTf, complex [{IrCl[κ^3-*N*,*C*,*N*-(pyC$_6$HMe$_2$py)]}(μ-Cl)]$_2$ (**1**; pyC$_6$H$_2$Me$_2$py = 1,3-di(2-pyridyl)-4,6-dimethylbenzene) reacts with 9-(6-phenylpyridin-2-yl)-9*H*-carbazole (PhpyCzH) and 2-phenoxy-6-phenylpyridine (PhpyOPh) to give [Ir{κ^3-*N*,*C*,*N*-(pyC$_6$HMe$_2$py)}{κ^3-*C*,*N*,*C'*-(C$_6$H$_4$pyCzH)}]OTf (**2**) and [Ir{κ^3-*N*,*C*,*N*-(pyC$_6$HMe$_2$py)}{κ^3-*C*,*N*,*C'*-(C$_6$H$_4$pyOPh)}]OTf (**3**). The X-ray diffraction structures of **2** and **3** reveal that the carbazolyl and phenoxy substituents of the *C*,*N*,*C'* ligand coordinate to the metal center to form an η^1-arene π-bond. Treatment of **2** and **3** with KO*t*Bu produces the deprotonation of the coordinated carbon atom of the η^1-arene group to afford the molecular phosphorescent [5t+4t']-heteroleptic iridium(III) complexes Ir{κ^3-*N*,*C*,*N*-(pyC$_6$HMe$_2$py)}{κ^3-*C*,*N*,*C'*-(C$_6$H$_4$pyCz)} (**4**) and Ir{κ^3-*N*,*C*,*N*-(pyC$_6$HMe$_2$py)}{κ^3-*C*,*N*,*C'*-(C$_6$H$_4$pyOC$_6$H$_4$)} (**5**). They are green emitters, which display short lifetimes and high quantum yields of 0.73 (**4**) and 0.87 (**5**) in the solid state.

Introduction

Metal-arene binding is a topic of general interest in chemistry. Among the found interactions, the η^1-coordination is one of the least common forms.[1] η^1-Arene complexes are grouped into two extreme classes: σ- and π-complexes,[2] although a continuous transition between both types of species is observed.[3] These groups are established by means of differences in structural features, mainly through the α and β angles (Chart 1). σ-Complexes display similar α and β angles, which are close to 55º as a result of a significant rehybridization of the coordinated carbon from sp^2 to sp^3. Hard cations favor this class of compounds.[4] In contrast, softer ions form π-complexes, which are characterized by a β angle close to 90º, an α angle close to 0º, and largely unperturbed arene rings from both structural and spectroscopic points of view.[5] The rehybridization of the coordinated atom in σ-complexes results in a positive charge in the aromatic ring, which activates towards nucleophilic attack. The coordination effect on the reactivity of the arene has been scarcely studied in π-complexes and nothing is known about the behavior of these species in the presence of nucleophiles or bases.

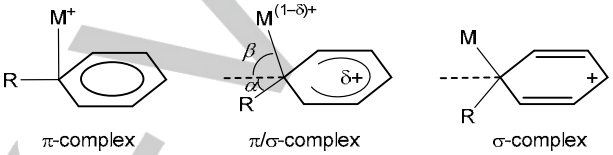

Chart 1. Types of η^1-coordinated arene complexes showing the angles between the arene plane and the *ipso*-substituent (α) and metal (β), respectively.

Carbazole is an aromatic heterocyclic moiety, consisting of two benzene rings fused on either side of a five-membered nitrogen-containing ring. Carbazole derivatives display good hole-transporting ability and possess large triplet energy. As a consequence of that, they are widely used as host materials in the preparation of phosphorescent organic light-emitting diodes (PHOLEDs).[6] In addition, hole-transporting carbazole groups have been introduced into the core of a ligand coordinated to the phosphorescent transition metal emitter, in order to reduce the energy barrier height for the hole injection and to decrease the triplet-triplet annihilation. Four approaches have been developed: (i) direct use of carbazole as amide ligands to form homoleptic low coordinate transition metal complexes;[7] (ii) carbazolide groups used as central anionic linker in CNC-,[8] PNP-,[9] and NNN-pincer based[10] on bis(NHC), bis(phosphine), and bis(imino) ligands; (iii) chelate-supported metalated carbazole groups forming five-[11] and six- membered[12] heterometallarings; and (iv) carbazole groups used as peripheral arylamine substituents of coordinated bidentate ligands in homoleptic and heteroleptic complexes.[13] However, as far as we know, complexes containing a carbazole group coordinated as η^1-arene are unprecedented.

There is a growing interest in phosphorescent iridium(III) complexes because it appears to be possible to design heteroleptic species with bespoke excited-state properties, according to the requirements of a given application.[14] Some salts have been employed in light-emitting electrochemical cells (LECs)[15] and for OLED applications.[16] However, neutral compounds seem to be better emitters for device fabrication.[17] Thus, molecular iridium(III) derivatives are awaking more interest than iridium(III) salts. Most studies have focused on complexes containing two or three bidentate ligands.[18]

[a] Prof. Dr. M. A. Esteruelas, D. Gómez-Bautista, Prof. Dr. A. M. López, Dr. E. Oñate
Departamento de Química Inorgánica, Instituto de Síntesis Química y Catálisis Homogénea (ISQCH), Centro de Innovación en Química Avanzada (ORFEO-CINQA)
Universidad de Zaragoza - CSIC, 50009 Zaragoza, Spain
E-mail: maester@unizar.es
[b] Dr. J.-Y. Tsai, Dr. Xia
Universal Display Corporation
375 Phillips Boulevard, Ewing, New Jersey 08618, United States.

Supporting information for this article is given via a link at the end of the document.((Please delete this text if not appropriate))

Complexes with tridentate ligands have received less attention, although they can be also tailored to express specific luminescent properties and they further generate less ligands redistribution issues. The stabilization of neutral heteroleptic iridium(III) complexes of this class implies the coordination of both a formal monoanionic tridentate ligand and a formal dianionic tridentate group. The four heterometallacyces formed in the resulting [5t+4t'][19] complexes are usually five-membered.[20] Recently, Wu, Fox, Chi, and co-workers have reported complexes with one six-membered heterometallacycle.[17g]

In the search for new molecular heteroleptic emitters of iridium(III), we decided to replace one of the phenyl substituents of 2,6-diphenylpyridine by carbazol-9-yl and phenoxy groups (Chart 2), in order to prepare [5t+4t'] complexes with one six-membered heterometallaring in their structure. 9-(6-Phenylpyridin-2-yl)-9*H*-carbazole (PhpyCzH) was prepared by Kim, Yoon, and coworkers in 2011,[21] although its reactivity with metals has not been studied, whereas 2-phenoxy-6-phenylpyridine (PhpyOPh) was described by Luo, Hu, and coworkers in 2013[22] and it has proved to favor nonclassical interactions in the chemistry of transition metal polyhydrides.[23] During the preparation of the target compounds, we have discovered novel η^1-arene intermediates involving the carbazolyl and phenoxy substituents of the pyridines. This paper reports the characterization of these intermediates, demonstrates that the coordination of the carbon atom to the metal cation produces an electrophilicity transfer from the metal to the Ir-CH hydrogen atom, and describes the photophysical properties of novel [5t+4t'] iridium complexes.

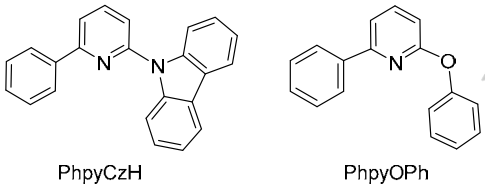

Chart 2. Tridentate ligands (4t') used in this study.

Results and Discussion

η^1-Arene intermediates

Williams and co-workers have previously reported that the iridium(III) dimer [{IrCl[κ^3-*N*,*C*,*N*-(pyC_6HMe_2py)]}(μ-Cl)]$_2$ (**1**; $pyC_6H_2Me_2py$ = 1,3-di(2-pyridyl)-4,6-dimethylbenzene) reacts with 2,6-diphenylpyridine, in the presence of silver trifluoromethanesulfonate (AgOTf), using molten 2,6-diphenylpyridine itself as the reaction solvent, to give the [5t+4t'] derivative Ir[κ^3-*N*,*C*,*N*-(pyC_6HMe_2py)][κ^3-*C*,*N*,*C*-($C_6H_4pyC_6H_4$)]. This compound is the result of the extraction of the chloride ligands of **1** and the *ortho*-CH activation of both substituents of the pyridine. It is obtained in moderate yield, about 40%, after chromatographic purification.[20a,b]

The formation of five-membered heterometallacycles certainly favors the C−H bond activation processes. Thus, in contrast to the phenyl substituents of 2,6-diphenylpyridine, the carbazole group of PhpyCzH and the phenoxy substituent of PhpyOPh do not undergo any C−H bond activation reaction under the same conditions. Thus, in the presence of 4.0 mol of AgOTf, the reaction of **1** with both pyridines, using the molten pyridine itself as the reaction solvent, lead to the salts [Ir{κ^3-*N*,*C*,*N*-(pyC_6HMe_2py)}{κ^3-*C*,*N*,*C'*-(C_6H_4pyCzH)}]OTf (**2**) and [Ir{κ^3-*N*,*C*,*N*-(pyC_6HMe_2py)}{κ^3-*C*,*N*,*C'*-(C_6H_4pyOPh)}]OTf (**3**), respectively, which were isolated as yellow solids in excellent yields of 89 and 87% (Scheme 1) and characterized by X-ray diffraction analysis.

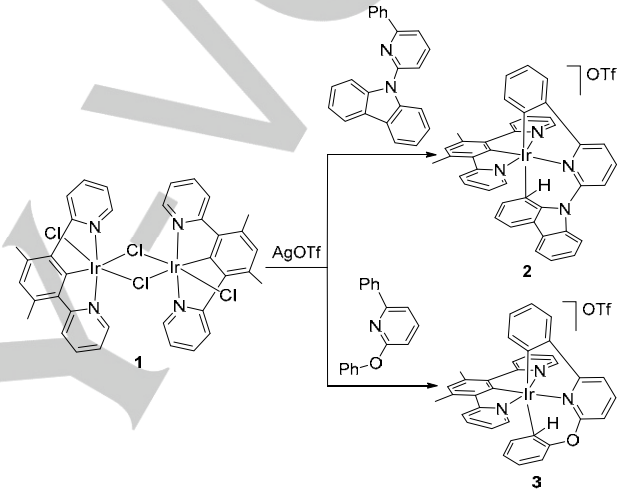

Scheme 1. Formation of η^1-arene complexes **2** and **3**.

The structure of **2** has two cations and two anions chemically equivalent but crystallographically independent in the asymmetric unit. Figure 1 shows a drawing of one of the cations. The abstraction of the chloride ligands of **1** generates three unoccupied coordination positions at the metal center, which allows the coordination of the phenyl and carbazole substituents of the pyridine. The coordination of the phenyl group facilitates the heterolytic cleavage of one of its *ortho*-CH bonds by using other PhpyCzH molecule as external base;[24] the leading force for this activation appears to be the stability of the formed five-membered heterometallacycle (N1−Ir1−C1 = 80.1(7) and 78.8(7)º), which has no counterpart with any C−H bond activation reaction on the carbazole group. As a consequence, the structural integrity of the carbazole substituent is maintained after the coordination. The carbazole binds the metal center through its C^1 atom (C13 in Figure 1) to form an η^1-arene π-complex, which displays Ir1−C13 bond lengths of 2.47(2) and 2.41(2) Å whereas the separations between the iridium center and the hydrogen atom bonded to C13 (H13) of 2.468 and 2.411 Å are significantly longer than those expected for an agostic interaction (1.8−2.2 Å).[25] In agreement with this, the Ir−H13−C13 angles of 77 and 82º, which compare well with

those found by Berman and Tilley for a series of η^1-arene-rhodium(III) complexes with bis(oxazoline)-4,6-dimethylbenzene ligands (74−78º),[5f] are more acute than the expected ones for an agostic interaction (90−130º).[25,26] The π-nature of the η^1-arene bond is strongly supported by the β and α angles, which exhibit values of 73.5 and 1º for one of the cations and 79.5 and 5.6º for the other one. In agreement with the η^1-coordination, the separation between the metal center and the adjacent carbons to the coordinated atom, C12 and C14, of 2.85(2) and 2.90(2) and 3.00(2) and 2.95(2), respectively for **2** and 2.920(4) and 2.782(4), respectively, for **3** are between 0.3 and 0.6 Å longer than the Ir–C13 bond lengths; consequently, the parameters ρ_1 and ρ_2 of 1.15 and 1.20 and 1.21 and 1.22 for **2** and 1.20 and 1.14 for **3**, calculated according to equations 1 and 2,[1] are similar and higher than 1. The metal center, the coordinated carbazole substituent, and the disubstituted pyridyl group form a six-membered heterometallaring with C13−Ir1−N1 angles of 82.9(7) and 82.7(7)º. The polyhedron around the iridium atom, resulting from the coordination of the *N*,*C*,*N*- and *C*,*N*,*C'*-pincer ligands, can be rationalized as a distorted octahedron with C−Ir−C', N−Ir−C, and N−Ir−N angles of 158.5(7) and 158.9(7)º (C1−Ir1−C13), 174.3(7) and 173.1(7)º (N1−Ir1−C30), and 161.9(7) and 160.1(6)º (N3−Ir1−N4), respectively.

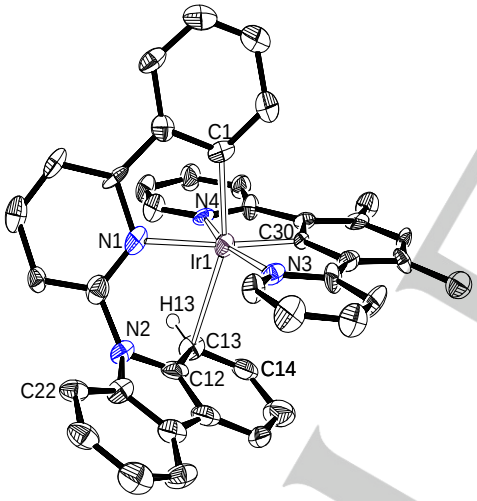

Figure 1. ORTEP diagram of one of the two independent cations of **2** in the asymmetric unit (50% probability ellipsoids). Hydrogen atoms (except H13) are omitted for clarity. Selected bond lengths (Å) and angles (deg) for both cations: Ir1–C1 = 2.002(18), 1.99(2), Ir1–C13 = 2.47(2), 2.41(2), Ir1–C30 = 1.941(16), 1.934(19), Ir1–N1 = 2.155(16), 2.195(17), Ir1–N3 = 2.036(14), 2.042(14), Ir1–N4 = 2.066(14), 2.045(15), Ir1···H13 = 2.468, 2.411; C1–Ir1–C13 = 158.5(7), 158.9(7), N1–Ir1–C13 = 82.9(7), 82.7(7), N1–Ir1–C1 = 80.1(7), 78.8(7), N3–Ir1–N4 = 161.9(7), 160.1(6), C30–Ir1–N3 = 79.7(7), 81.1(8), C30–Ir1–N4 = 82.2(6), 79.0(8), C30–Ir1–N1 = 174.3(7), 173.1(7).

$$\rho_1 = \text{Ir–C12 / Ir–C13} \quad (1)$$
$$\rho_2 = \text{Ir–C14 / Ir–C13} \quad (2)$$

The $^{13}C\{^1H\}$ and ^1H NMR spectra of the salt, in [D_2]dichloromethane, at room temperature suggest that the η^1-arene bond is kept in solution, although the iridium center is involved in a dynamic position exchange process between the C13 and C22 carbon atoms of the carbazole. Thus, the $^{13}C\{^1H\}$ spectrum shows a relatively high field resonance[27] at δ 97.9, which appear as a broad singlet, for the inequivalent C13 and C22 atoms, whereas the ^1H NMR spectrum also contains only one signal at δ 7.58 for the H13 and H22 atoms bonded to C13 and C22, respectively. Singlets at δ 177.1 and 133.3 for the aryl metalated carbon atoms C30 and C1, respectively, in the $^{13}C\{^1H\}$ NMR spectrum are also characteristic spectroscopic features of the cation of **2**.

Figure 2 shows a view of the cation of **3**. The structure demonstrates that it is a phenoxy counterpart of **2**. The disubstituted pyridine undergoes the *ortho*-CH bond activation of the phenyl substituent and the η^1-arene coordination of one of the *ortho* carbon atoms of the phenoxy substituent. As a result, the coordination polyhedron around the iridium atom can be rationalized as that of **2** with the phenoxy group in the position of the carbazole and C−Ir−C', N−Ir−C, and N−Ir−N angles of 158.56(14)º (C1−Ir−C13), 170.25(14)º (N1−Ir−C30), and 160.94(12)º (N2−Ir−N3), respectively. The Ir−C13 bond length of 2.437(4) Å compares well with that found in the carbazole derivative, whereas the separation between the metal center and the hydrogen atom bonded to C13 (H13) of 2.779 Å is even 0.3 Å longer. In this case, the β and α angles exhibit values of 83.5 and 18.1º, respectively. The $^{13}C\{^1H\}$ and ^1H NMR spectra of this salt, in [D_2]dichloromethane, are consistent with the π-coordination of C13 to the iridium atom, which, even at 233 K, moves fast between the two *ortho* carbon atoms of the phenoxy group (C13 and C17). Thus, the $^{13}C\{^1H\}$ NMR spectrum shows a signal at δ 121.7 for both inequivalent carbon atoms, whereas the resonances corresponding to the metalated aryl carbons C1 and C30 appear at δ 137.5 and 177.4, respectively. In agreement with the $^{13}C\{^1H\}$ ^1H NMR spectrum, the ^1H NMR spectrum displays only one resonance at δ 7.34 for the inequivalent *ortho* hydrogen atoms of the phenoxy group, H13 and H17.

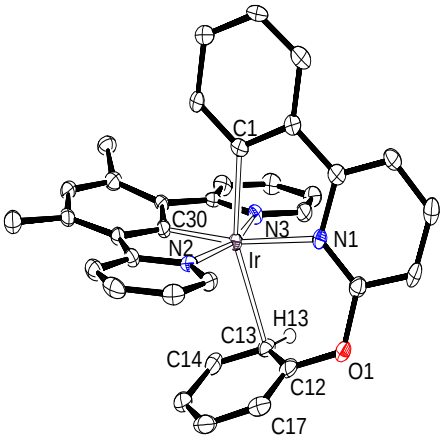

Figure 2. ORTEP diagram of the cation of **3** (50% probability ellipsoids). Hydrogen atoms (except H13) are omitted for clarity. Selected bond lengths (Å) and angles (deg): Ir–C1 = 2.003(4), Ir–C13 = 2.437(4), Ir–C30 = 1.947(4), Ir–N1 = 2.211(3), Ir–N2 = 2.038(3), Ir–N3 = 2.060(3), Ir···H13 = 2.779; C1–Ir–C13 = 158.56(14), N1–Ir–C13 = 80.92(13), N1–Ir–C1 = 79.75(13), N2–Ir–N3 =

160.94(12), C30–Ir–N2 = 80.45(13), C30–Ir–N3 = 80.54(13), C30–Ir–N1 = 170.25(14).

Deprotonation of the hydrogen atom bonded to the coordinated carbon atom: formation of [5t+4t'] complexes bearing a six-membered heterometallacycle

The *π*-coordination of the metal center to the C(13) carbon atom of the carbazolyl and phenoxy groups of **2** and **3** does not appear to disturb the aromaticity of the coordinated cycle, which display similar C–C bond lengths and angles along the ring. However, it enhances the acidity of the H13 hydrogen atom, as a result of an electrophilicity transfer from the metal cation to the C13–H13 bond. Thus, at room temperature, the addition of 4.0 equiv of potassium tert-butoxide (KO*t*Bu) to tetrahydrofuran solutions of **2** and **3** produces the deprotonation of the coordinated carbon atom and the formation of the [5t+4t'] complexes Ir{κ^3-*N*,*C*,*N*-(pyC$_6$HMe$_2$py)}{κ^3-*C*,*N*,*C'*-(C$_6$H$_4$pyCz)} (**4**) and Ir{κ^3-*N*,*C*,*N*-(pyC$_6$HMe$_2$py)}{κ^3-*C*,*N*,*C'*-(C$_6$H$_4$pyOC$_6$H$_4$)} (**5**), respectively, according to Scheme 2. The reactions are reversible. The addition of HOTf to dichloromethane solutions of **4** and **5** regenerates the salts **2** and **3**.

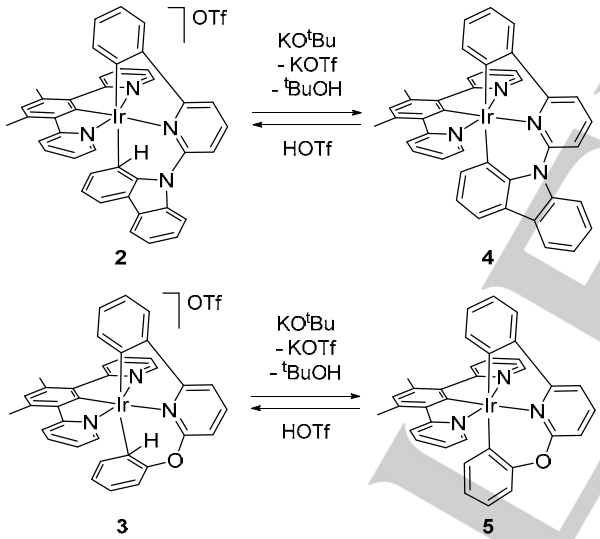

Scheme 2. Formation of neutral [5t+4t´] complexes **4** and **5**.

The formation of the new [5t+4t´] complexes is strongly supported by the X-ray diffraction structure of **5** (Figure 3), which proves the deprotonation of the coordinated carbon atom C13 of **3** and the formation a new dianionic *C*,*N*,*C'*-pincer ligand (4t'). The deprotonation generates a strong iridium-aryl bond with an Ir–C13 bond length of 2.095(4) Å, which is statistically identical to the Ir–C1 distance of 2.078(4) Å and about 0.2 Å longer than the Ir–C30 bond length of 1.918(4) Å. The coordination of the resulting *C*,*N*,*C'*-pincer ligand gives rise to a five-membered heterometallaring with a N1–Ir–C1 angle of 79.13(14)º, which is similar to that of **3** (79.75(13)), and a six-membered heterometallacycle with a N1–Ir–C13 angle of 88.56(14)º, which is very close to the ideal value of 90º for an iridium(III) complex. The generated coordination polyhedron around the iridium atom can be described as the expected distorted octahedron with C–Ir–C', N–Ir–C, and N–Ir–N angles of 166.92(16)º (C1–Ir–C13), 176.13(14) (N1–Ir–C30), and 161.13(13) (N2–Ir–N3), respectively.

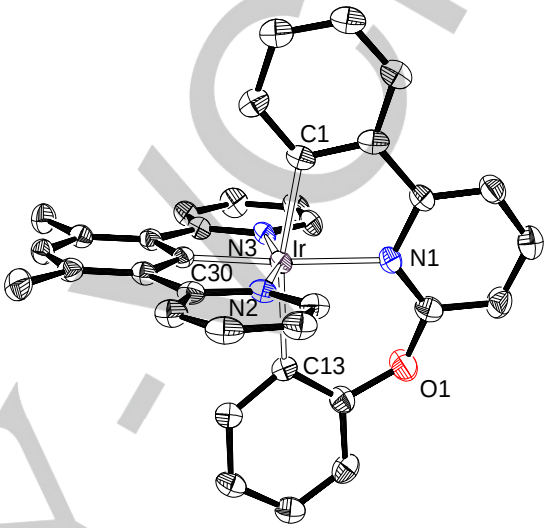

Figure 3. ORTEP diagram of 5 (50% probability ellipsoids). Hydrogen atoms are omitted for clarity. Selected bond lengths (Å) and angles (deg): Ir–C1 = 2.078(4), Ir–C13 = 2.095(4), Ir–C30 = 1.918(4), Ir–N1 = 2.145(3), Ir–N2 = 2.043(3), Ir–N3 = 2.044(3); C1–Ir–C13 = 166.92(16), N1–Ir–C13 = 88.56(14), N1–Ir–C1 = 79.13(14), N2–Ir–N3 = 161.13(13), C30–Ir–N2 = 80.42(15), C30–Ir–N3 = 80.71(15), C30–Ir–N1 = 176.13(14).

The $^{13}C\{^1H\}$ and ^1H NMR spectra of **4** and **5**, in [D$_2$]dichloromethane, at room temperature, are consistent with the structure shown in Figure 3. The resonances corresponding to the metalated carbon atoms appear at δ 189.6 (C$_6$HMe$_2$), 171.9 (C$_6$H$_4$), and 141.1 (Cz) for **4** and at δ 191.0 (C$_6$HMe$_2$), 170.4 (C$_6$H$_4$), and 138.1 (OC$_6$H$_4$) for **5**.

Photophysical Properties of Complexes 4 and 5

UV/vis absorption data of 2.5 x 10^{-5} M 2-methyltetrahydrofuran solutions of the molecular complexes **4** and **5**, at room temperature, are collected in Table 1. The spectra of both complexes are similar (Figures S13 and S14 in the Supporting Information), showing three different zones: < 300, 300–440, and >440 nm. Time-dependent DFT calculations (B3LYP-GD3//SDD(f)/6-31G**), computed in tetrahydrofuran, indicate that the more intense absorptions at the highest energy region correspond mainly to $^1\pi$–π* interligand and intraligand transitions. The bands in the zone of moderate energy correspond to allowed spin metal-to-ligand charge transfer (^{1}MLCT) mixed with ligand-centered transitions. Thus, the absorptions at 440 nm for **4** and 432 nm for **5** are caused by a HOMO → LUMO transition. The HOMO is located at the metal

Table 1. Selected experimental UV-Vis absorptions of **4** and **5** (in 2-Me THF) and computed TD-DFT (in THF) vertical excitation energies and their major contributions.

Complex	λ_{exp} (nm)	ε ($M^{-1}\cdot cm^{-1}$)	Excitation energy (nm)	Oscillator strength (*f*)	Transition	Contribution (%)
4	278	41920	278	0.1005	HOMO-3 → LUMO+4	64
	318	18640	317	0.1346	HOMO-2 → LUMO+3	84
	374	9040	374	0.0826	HOMO-2 → LUMO	85
	440	3960	440	0.0839	HOMO → LUMO	92
	502	1320				
5	300	14600	300	0.1503	HOMO-4 → LUMO+2	59
					HOMO-5 → LUMO	16
	344	6240	343	1.1055	HOMO-2 → L+1	75
					HOMO → L+3	12
	432	3240	432	0.1208	HOMO → LUMO	92
	496	1200				

and both ligands (32% Ir + 27% *N*,*C*,*N* + 41% *C*,*N*,*C'* for **4** and 36% Ir + 44% *N*,*C*,*N* + 20% *C*,*N*,*C'* for **5**), while the LUMO is mainly centered on the pincer *N*,*C*,*N* ligand (88% for **4** and 92% for **5**). The weak absorption tails after 440 nm are usually assigned to formally spin-forbidden ^{3}MLCT transitions, caused by the large spin-orbit coupling introduced by the iridium center.[28]

Complexes **4** and **5**, are green emissive after photoexcitation in the solid state at room temperature and in 2-methyltethahydrofuran at room temperature and at 77 K, displaying bands centered between 515 and 555 nm. Figure 4 depicts the emission spectra whereas Table 2 summarizes calculated and experimental wavelengths, lifetimes, and quantum yields. The emissions can be attributed to T_1 excited stated states originated by HOMO → LUMO charge transfer transitions. In accordance with this, good agreement is observed between the experimental wavelengths and those calculated by estimating the difference in energy between the optimized triplet state T_1 and the singlet state S_0, in tetrahydrofuran. The lifetimes lie in the range of 1–10 μs, whereas the quantum yields, measured in the solid state in a doped poly(methylmethacrylate) (PMMA) film at 5 wt %, are 0.73 for **4** and 0.87 for **5**. The spectra in 2-methyltetrahydrofuran at 77 K shows that the emission is split into two bands, under these conditions. This is consistent with a change of the dominant character of the excited state from MLCT to ligand centered *π*–*π**.[29]

Conclusions

This study has revealed that the replacement of a phenyl substituent of 2,6-diphenyl pyridine by a carbazol-9-yl or phenoxy group gives rise to disubstituted pyridines, which are useful to form dianionic *C*,*N*,*C*'-pincer ligands by means of the heterolytic C–H bond activation of both substituents of the pyridine. The cleavage of the C–H bond of the carbazolyl and phenoxy groups takes place through an η^1-arene coordination of these substituents and affords a six-membered heterometallacycle with a N−Ir−C' angle close to 90º. This ability of the pyridines 9-(6-phenylpyridin-2-yl)-9*H*-carbazole and 2-phenoxy-6-phenylpyridine allows to prepare novel molecular phosphorescent [5t+4t']-heteroleptic iridium(III) dopants for OLEDs with one six-membered heterometallacyle in their structure. They are green emitters, which display short lifetimes and high quantum yields.

Table **2.** Photophysical data of complexes **4** and **5**

Complex	Calcd λ_{em}[a] (nm)	Media (T/K)	λ_{em} (nm)	λ_{exc} (nm)	τ[b] (μs)	Φ[c]
4	554	Powder (298)	528	374	2.1	0.73
		2-MeTHF (298)	555	378	2.0	
		2-MeTHF (77)	515, 548	379	10.1	
5	550	Powder (298)	524	422	1.3	0.87
		2-MeTHF (298)	539	420	7.7	
		2-MeTHF (77)	516, 545	416	5.9	

[a] In THF. [b] Measurements at λ_{max}. [c] Measurements in doped PMMA films at 5 wt %.

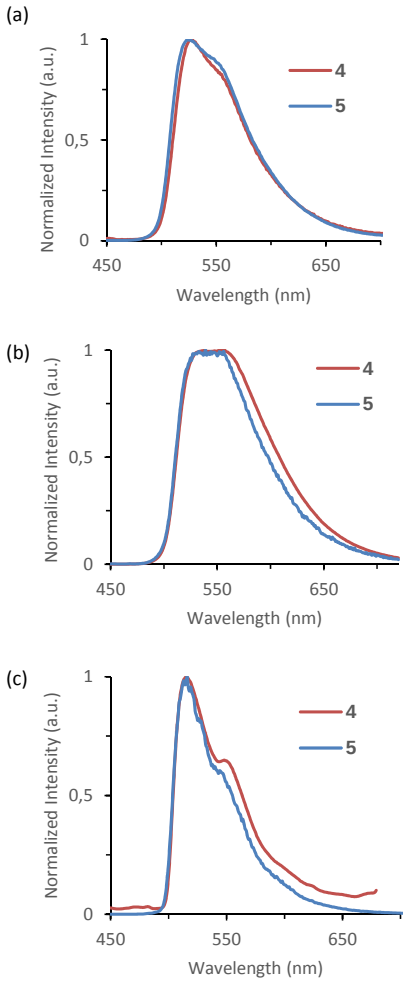

Figure 4. Emission spectra in neat solid powders at 298 K (a), in 2-MeTHF at 298 K (b), and in 2-MeTHF at 77 K (c) for complexes **4** and **5**.

Experimental Section

General Information. All reactions were carried out with rigorous exclusion of air using Schlenk-tube techniques. Solvents (except THF, 2-MeTHF, and MeOH which were dried and distilled under argon) were obtained oxygen- and water-free from an MBraun solvent purification apparatus. ^{1}H and ^{13}C{^{1}H} NMR spectra were recorded on Bruker Avance 400 MHz instrument. Chemical shifts (expressed in parts per million) are referenced to residual solvent peaks. Coupling constants *J* are given in hertz. C, H, and N analyses were carried out in a Perkin-Elmer 2400 CHNS/O analyzer. High-resolution electrospray mass spectra were acquired using a MicroTOF-Q hybrid quadrupole time-of-flight spectrometer (Bruker Daltonics, Bremen, Germany). UV-visible spectra were registered on an Evolution 600 spectrophotomer. Steady-state photoluminescence spectra were recorded on a Jobin-Yvon Horiba Fluorolog FL-3-11 spectrofluorimeter. Lifetimes were measured using an IBH 5000F coaxial nanosecond flash lamp. Quantum yields were measured using the Hamamatsu Absolute PL Quantum Yield Measurement System C11347-11. 9-(6-Phenylpyridin-2-yl)-9*H*-carbazole,[21] 2-phenoxy-6-phenylpyridine,[22] and [{IrCl[κ^3-*N*,*C*,*N*-(pyC_6HMe$_2$py)]}(μ-Cl)]$_2$ (**1**)[20a,b] were prepared by the published methods.

Preparation of [Ir{κ^3-*N*,*C*,*N*-(pyC_6HMe$_2$py)][κ^3-*C*,*N*,*C'*-(C_6H_4pyCzH)}]OTf (2).

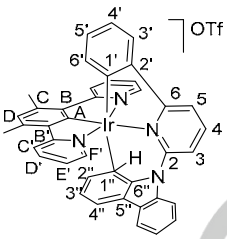

Complex **1** (100 mg, 0.096 mmol), AgOTf (99 mg, 0.384 mmol), and 9-(6-phenylpyridin-2-yl)-9*H*-carbazole (892 mg, 2.784 mmol) were heated at 110 ºC with stirring in a Schlenk flask equipped with a Teflon stopcock, for 24 h, in the darkness. After cooling to room temperature, the product was extracted with ethanol (2 x 5 mL). The solution was filtered through Celite to remove the silver salts. The resulting solution was concentrated and a greenish yellow solid precipitated by addition of diethyl ether (10 mL). This solid was washed with ether (3 x 8 mL) to remove the excess of 9-(6-phenylpyridin-2-yl)-9*H*-carbazole. Yield: 157 mg (89 %). Elemental analysis calcd (%) for $C_{42}H_{30}F_3IrN_4O_3S$: C, 54.83; H, 3.29; N, 6.09; S 3.49; found: C, 54.43; H, 3.50; N, 5.80; S, 3.49. HRMS (electrospray, *m*/*z*): calcd for $C_{41}H_{30}IrN_4$ [M$^+$]: 771.2097; found: 771.2217. ^{1}H NMR (400 MHz, CD_2Cl_2, 298 K): δ= 8.55 (dd, H, $^3J_{H\text{-}H}$ = $^3J_{H\text{-}H}$ = 8.0, H^4 py), 8.20 (m, 2H, H^3 + H^5 py), 8.01 (d, 2H, $^3J_{H\text{-}H}$ = 8.4, H$^{C'}$), 7.71 (dd, 2H, $^3J_{H\text{-}H}$ = 7.6, $^4J_{H\text{-}H}$ = 1.0, H$^{4''}$ Cz), 7.64 (ddd, 1H, $^3J_{H\text{-}H}$ = 8.4, $^3J_{H\text{-}H}$ = 7.5, $^4J_{H\text{-}H}$ = 1.7, H$^{D'}$), 7.61–7.56 (m, 3H, H$^{3'}$ C_6H_4 + H$^{1''}$ Cz), 7.04–6.97 (m, 5H, H$^{F'}$ + H^D + H$^{3''}$ Cz), 6.94 (ddd, 2H, $^3J_{H\text{-}H}$ = $^3J_{H\text{-}H}$ = 7.5, $^4J_{H\text{-}H}$ = 1.0, H$^{2''}$ Cz), 6.78 (ddd, 1H, $^3J_{H\text{-}H}$ = $^3J_{H\text{-}H}$ = 7.5, $^4J_{H\text{-}H}$ = 1.0, H$^{4'}$ C_6H_4), 6.55 (ddd, 2H, $^3J_{H\text{-}H}$ = 7.5, $^3J_{H\text{-}H}$ = 6.6, $^4J_{H\text{-}H}$ = 1.2, H$^{E'}$), 6.48 (ddd, 1H, $^3J_{H\text{-}H}$ = 7.9, $^3J_{H\text{-}H}$ = 7.5, $^4J_{H\text{-}H}$ = 1.5, H$^{5'}$ C_6H_4), 5.57 (dd, 1H, $^3J_{H\text{-}H}$ = 7.9, $^4J_{H\text{-}H}$ = 1.0, H$^{6'}$ C_6H_4), 2.82 (s, 6H, CH_3) ppm; ^{13}C{^{1}H} NMR (100 MHz, CD_2Cl_2, 298 K): δ= 177.1 (IrC^A), 168.9 (NC$^{B'}$), 163.5 (NC^6 py), 155.8 (NC^{2}N py), 151.7 (NC$^{F'}$), 144.0 (C$^{2'}$ C_6H_4), 142.7 (C^{4}H py), 142.4 (NC$^{6''}$ Cz), 138.9 (*C*^{C}Me), 138.8 (C^{D}H), 136.7 (C^B), 134.4 (C$^{6'}$H Ph), 133.3 (IrC$^{1'}$ C_6H_4), 132.1 (C$^{2''}$H Cz), 131.8 (C^{D}H), 131.0 (C$^{5'}$H C_6H_4), 126.2 (C$^{3'}$H C_6H_4), 126.0 (C$^{5''}$ Cz), 124.3 (C$^{4'}$H C_6H_4), 123.9 (C$^{C'}$H), 123.7 (C$^{4''}$H Cz), 122.8 (C$^{E'}$H), 122.6 (C$^{3''}$H cbz), 119.1 (C$^{3/5}$H py), 118.4 (C$^{3/5}$H py), 97.9 (C$^{1''}$H cbz), 22.8 (CH_3) ppm.

Preparation of [Ir{κ^3-*N*,*C*,*N*-(pyC_6HMe$_2$py)][κ^3-*C*,*N*,*C'*-(C_6H_4pyOPh)}]OTf (3).

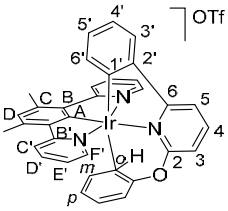

This complex was prepared as described for **2** starting from 100 mg (0.096 mmol) of **1**, 99 mg (0.384 mmol) of AgOTf, and 688 mg (2.784 mmol) of 2-phenoxy-6-phenylpyridine. A yellow solid was obtained. Yield: 141 mg (87%). Elemental analysis calcd (%) for $C_{36}H_{27}F_3IrN_3O_4S$: C 51.06, H 3.21, N 4.97, S 3.79; found: C 51.28, H 3.28, N 4.56, S 3.99. HRMS (electrospray, *m*/*z*): calcd for $C_{35}H_{27}IrN_3O$ [M$^+$]: 698.1783; found: 698.1790. ^{1}H NMR (400 MHz, CD_2Cl_2, 233 K): δ= 8.06 (d, 2H, $^3J_{H\text{-}H}$ = 8.0, H$^{C'}$), 7.97 (dd, 1H, $^3J_{H\text{-}H}$ = $^3J_{H\text{-}H}$ = 8.0, H^4 py), 7.91–7.86 (m, 3H, H$^{3/5}$ py + H$^{F'}$), 7.73 (ddd, 2H, $^3J_{H\text{-}H}$ = $^3J_{H\text{-}H}$ = 8.0, $^4J_{H\text{-}H}$ = 1.6, H$^{D'}$), 7.60 (dd, 1H, $^3J_{H\text{-}H}$ = 7.7, $^4J_{H\text{-}H}$ = 1.3, H$^{3'}$ C_6H_4), 7.51 (m, 2H, H^m OPh), 7.40–7.31 (m, 3H, H^p + H^o OPh), 7.00 (m, 3H, H$^{E'}$ + H^D), 6.76 (d, 1H, $^3J_{H\text{-}H}$ = 8.0, H$^{3/5}$ py), 6.73 (ddd, 1H, $^3J_{H\text{-}H}$ = $^3J_{H\text{-}H}$ = 7.7, $^4J_{H\text{-}H}$ = 1.1, H$^{4'}$ C_6H_4), 6.52 (ddd, 1H, $^3J_{H\text{-}H}$ = $^3J_{H\text{-}H}$ = 7.7, $^4J_{H\text{-}H}$ = 1.3, H$^{5'}$ C_6H_4), 6.00 (dd, 1H, $^3J_{H\text{-}H}$ = 7.7, $^4J_{H\text{-}H}$ = 1.1, H$^{6'}$ C_6H_4), 2.82 (s, 6H, CH_3) ppm; ^{13}C{^{1}H} NMR (100 MHz, CD_2Cl_2,

298 K): δ= 177.4 (IrC^{A}), 169.6 (NC$^{B'}$), 166.3 (NC^{2}O py), 162.8 (NC^{6} py), 152.6 (OC OPh), 152.2 (NC$^{F'}$H), 143.5 (C$^{2'}$ C_6H_4), 141.7 (C^{4}H py), 138.2 (C$^{D'}$H), 138.1 (*C*^{C}Me), 137.6 (C^{B}), 137.5 (IrC$^{1'}$ C_6H_4), 136.7 (C$^{6'}$H C_6H_4), 130.9 (C^{m}H OPh), 130.8 (C^{D}H), 129.3 (C$^{5'}$H C_6H_4), 127.2 (C^{p}H OPh), 125.0 (C$^{3'}$H C_6H_4), 123.5 (C$^{C'}$H), 122.7 (C$^{E'}$H), 122.0 (C$^{4'}$H C_6H_4), 121.7 (C^{o}H OPh), 114.2 (C$^{3/5}$H py), 108.0 (C$^{3/5}$H py), 22.6 (CH_3) ppm.

Preparation of Ir{κ^3-*N*,*C*,*N*-(pyC_6HMe$_2$py)}{κ^3-*C*,*N*,*C'*-(C_6H_4pyCz)} (4).

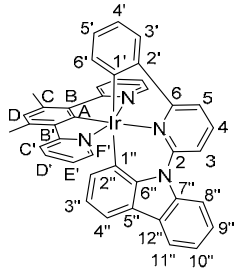

A solution of KO*t*Bu (77 mg, 0.686 mmol) in 5 mL of THF was slowly added via cannula (5-10 min) into a suspension of **2** (157 mg, 0.171 mmol) in 5 mL of THF. The yellow suspension changed to a red-brown solution and, after 2 h, a yellow-brown solid appeared. The solvent was removed in vacuo and the product was extracted with CH_2Cl_2 (3 x 4 mL). The resulting solution was concentrated and a yellow-orange solid precipitated by diethyl ether addition (8 mL). The solid was washed with a 1:2 dichloromethane/diethyl ether mixture (2 x 3 mL) and subsequently with pentane (3 x 8 mL). Yield: 51 mg (39%). Elemental analysis calcd (%) for $C_{41}H_{29}IrN_4$: C 63.96, H 3.80, N 7.28; found: C 63.67, H 3.66, N 7.64. HRMS (electrospray, *m/z*): calcd for $C_{41}H_{30}IrN_4$ [M$^+$+H]: 771.2099; found: 771.2094. ^{1}H NMR (400 MHz, CD_2Cl_2, 298 K): δ= 8.20 (dd, 1H, $^3J_{H\text{-}H}$ = 8.0, $^4J_{H\text{-}H}$ = 0.9, H$^{3/5}$ py), 8.18 (d, 1H, $^3J_{H\text{-}H}$ = 7.3, H$^{8''}$ C_6H_4-Cz), 8.14 (dd, 1H, $^3J_{H\text{-}H}$ = $^3J_{H\text{-}H}$ = 8.0, H^4 py), 8.07 (d, 2H, $^3J_{H\text{-}H}$ = 8.4, H$^{C'}$), 8.00 (dd, 1H, $^3J_{H\text{-}H}$ = 8.0, $^4J_{H\text{-}H}$ = 0.9, H$^{3/5}$ py), 7.96 (d, 1H, $^3J_{H\text{-}H}$ = 7.0, H$^{11''}$ C_6H_4-Cz), 7.80 (d, 1H, $^3J_{H\text{-}H}$ = 7.8, H$^{3'}$ C_6H_4), 7.63 (dd, 2H, $^3J_{H\text{-}H}$ = 5.8, $^4J_{H\text{-}H}$ = 1.0, H$^{F'}$), 7.46 (ddd, 1H, $^3J_{H\text{-}H}$ = 8.5, $^3J_{H\text{-}H}$ = 7.3, $^4J_{H\text{-}H}$ = 1.3, H$^{9''}$ C_6H_4-Cz), 7.44 (ddd, 2H, $^3J_{H\text{-}H}$ = 8.4, $^3J_{H\text{-}H}$ = 7.4, $^4J_{H\text{-}H}$ = 1.7, H$^{D'}$), 7.34–7.28 (m, 2H, H$^{4''}$ C_6H_3-Cz + H$^{10''}$ C_6H_4-Cz), 7.04 (s, 1H, H^{D}), 6.81 (ddd, 1H, $^3J_{H\text{-}H}$ = 7.2, $^4J_{H\text{-}H}$ = 1.2, H$^{4'}$, C_6H_4), 6.61 (ddd, 1H, $^3J_{H\text{-}H}$ = $^3J_{H\text{-}H}$ = 7.2, $^4J_{H\text{-}H}$ = 1.1, H$^{5'}$ C_6H_4), 6.58–6.51 (m, 3H, H$^{3''}$ C_6H_3-Cz + H$^{E'}$), 6.19 (dd, 1H, $^3J_{H\text{-}H}$ = 7.4, $^4J_{H\text{-}H}$ = 1.4, H$^{2''}$ C_6H_3-Cz), 6.18 (dd, 1H, $^3J_{H\text{-}H}$ = 7.2, $^4J_{H\text{-}H}$ = 1.2, H$^{6'}$ C_6H_4), 2.96 (s, 6H, CH_3) ppm; ^{13}C{^{1}H} NMR (100 MHz, CD_2Cl_2, 298 K): δ= 189.6 (IrC^{A}), 171.9 (IrC$^{1'}$ C_6H_4), 168.8 (NC$^{B'}$), 168.1 (NC^{6} py), 150.8 (NC$^{F'}$H), 150.5 (NC^{2}N py), 146.2 (C$^{2'}$ C_6H_4), 144.7 (NC$^{6''}$ Cz), 141.1 (IrC$^{1''}$ Cz), 139.9 (NC$^{7''}$ Cz), 138.3 (C^{4}H py), 138.2 (C$^{2''}$H C_6H_3-Cz), 138.0 (C$^{6'}$H C_6H_4), 137.5 (C^{C}), 136.0 (C^{B}), 134.5 (C$^{D'}$H), 129.7 (C$^{12''}$ C_6H_4-Cz), 128.8 (C$^{5'}$H Ph), 127.4 (C^{D}H), 125.1 (C$^{3'}$H C_6H_4), 124.9 (C$^{9''}$H C_6H_4-Cz), 123.0 (C$^{C'}$H), 122.4, 122.4 (C$^{3''}$H + C$^{4''/10''}$H Cz), 121.9 (C$^{4'}$H C_6H_4), 121.3 (C$^{E'}$H), 121.0 (C$^{5''}$ C_6H_3-Cz), 120.8 (C$^{11''}$H C_6H_4-Cz), 115.4 (C$^{8''}$H C_6H_4-Cz), 114.6 (C$^{3/5}$H py), 113.3 (C$^{3/5}$H py), 113.3 (C$^{4''/10''}$H Cz), 23.0 (CH_3) ppm.

Preparation of Ir{κ^3-*N*,*C*,*N*-(pyC_6HMe$_2$py)}{κ^3-*C*,*N*,*C'*-(C_6H_4pyOC_6H_4)} (5).

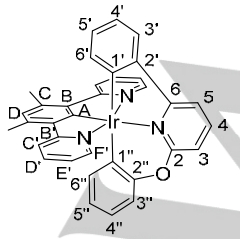

This complex was prepared as described for **4** starting from 141 mg (0.158 mmol) of **3** and 71 mg (0.632 mmol) of KO*t*Bu. A yellow-orange solid was obtained. Yield: 66 mg (56 %). Elemental analysis calcd (%) for $C_{35}H_{26}IrN_3O$: C 60.33, H 3.76, N 6.03; found: C 60.20, H 3.89, N 5.88. HRMS (electrospray, *m/z*): calcd for $C_{35}H_{27}IrN_3O$ [M$^+$+H]: 698.1783; found: 698.1786. ^{1}H NMR (400 MHz, CD_2Cl_2, 298 K): δ= 8.08 (d, 2H, $^3J_{H\text{-}H}$ = 8.2, H$^{C'}$), 8.07 (dd, 1H, $^3J_{H\text{-}H}$ = $^3J_{H\text{-}H}$ = 8.0, H^4 py), 7.88 (dd, 1H, $^3J_{H\text{-}H}$ = 8.0, $^4J_{H\text{-}H}$ = 0.9, H^5 py), 7.73 (dd, 1H, $^3J_{H\text{-}H}$ = 7.5, $^4J_{H\text{-}H}$ = 1.2, H$^{3'}$ C_6H_4), 7.69 (ddd, 2H, $^3J_{H\text{-}H}$ = 5.8, $^4J_{H\text{-}H}$ = 1.7, $^5J_{H\text{-}H}$ = 0.8, H$^{F'}$), 7.48 (ddd, 2H, $^3J_{H\text{-}H}$ = 8.2, $^3J_{H\text{-}H}$ = 7.8, $^4J_{H\text{-}H}$ = 1.7, H$^{D'}$), 7.32 (dd, 1H, $^3J_{H\text{-}H}$ = 8.0, $^4J_{H\text{-}H}$ = 0.9, H^3 py), 7.03 (s, 1H, H^{D}), 6.94 (dd, 1H, $^3J_{H\text{-}H}$ = 8.0, $^4J_{H\text{-}H}$ = 1.2, H$^{3''}$ OC_6H_4), 6.74 (ddd, 1H, $^3J_{H\text{-}H}$ = 7.5, $^4J_{H\text{-}H}$ = 1.4, H$^{4'}$ C_6H_4), 6.65–6.59 (m, 3H, H$^{E'}$ + H$^{4''}$ OC_6H_4), 6.55 (ddd, 1H, $^3J_{H\text{-}H}$ = $^3J_{H\text{-}H}$ = 7.2, $^4J_{H\text{-}H}$ = 1.2, H$^{5'}$ C_6H_4), 6.28 (ddd, 1H, $^3J_{H\text{-}H}$ =$^3J_{H\text{-}H}$ = 7.2, $^4J_{H\text{-}H}$ = 1.2, H$^{5''}$ OC_6H_4), 6.14 (dd, 1H, $^3J_{H\text{-}H}$ = 7.2, $^4J_{H\text{-}H}$ = 1.9, H$^{6''}$ OC_6H_4), 6.09 (dd, 1H, $^3J_{H\text{-}H}$ = 7.2, $^4J_{H\text{-}H}$ = 1.4, H$^{6'}$ C_6H_4), 2.95 (s, 6H, CH_3) ppm; ^{13}C{^{1}H} NMR (100 MHz, CD_2Cl_2, 298 K): δ= 191.0 (IrC^{A}), 170.4 (IrC$^{1'}$ C_6H_4), 168.4 (NC$^{B'}$), 166.0 (NC^{6} py), 158.0 (NC^{2}O py), 154.6 (OC$^{2''}$ OC_6H_4), 149.9 (NC$^{F'}$H), 144.5 (C$^{2'}$ C_6H_4), 140.7 (C$^{6''}$H OC_6H_4), 139.0 (C^{4}H py), 138.1 (IrC$^{1''}$ OC_6H_4), 137.8 (C$^{6'}$H C_6H_4), 137.0 (C^{B}), 135.5 (C^{C}), 134.1 (C$^{D'}$H), 128.3 (C$^{5'}$H C_6H_4), 126.8 (C^{D}H), 124.1 (C$^{3'}$H C_6H_4), 123.0 (C$^{5''}$H OC_6H_4), 122.7 (C$^{4''}$H OC_6H_4), 122.5 (C$^{C'}$H), 121.3 (C$^{4'}$H C_6H_4), 120.6 (C$^{E'}$H), 115.1 (C$^{3''}$H OC_6H_4), 113.2 (C^{5}H py), 111.2 (C^{3}H py), 22.4 (CH_3) ppm.

Structural Analysis of Complexes 2, 3, and 5. Single crystals were grown from a saturated solution in fluorobenzene at 243 K (**2**), by slow diffusion of diethyl ether into a dichloromethane solution at 243 K (**3**), and by slow evaporation of a dichloromethane solution at 298 K (**5**). X-ray data were collected on a Bruker Smart APEX DUO (**3**) or Bruker Smart APEX CCD (**2**, **5**) diffractometer equipped with a normal focus, 2.4 kW sealed tube source (Mo radiation, λ = 0.71073 Å) operating at 50 kV and 30 mA (**5**) or 40 mA (**2**, **3**). Data were collected over the complete sphere. Each frame exposure time was 10 s (**5**), 20 s (**2**), or 30 s (**3**) covering 0.3^o in ω. Data were corrected for absorption by using a multiscan method applied with the SADABS program.[30] The structures were solved by Patterson or direct methods and refined by full-matrix least squares on F^2 with SHELXL2016,[31] including isotropic and subsequently anisotropic displacement parameters. The hydrogen atoms were observed in the least Fourier Maps or calculated, and refined freely or using a restricted riding model. CCDC 1553073 (**2**), 1553074 (**3**), and 1553075 (**5**) contain the supplementary crystallographic data for this paper. These data are provided free of charge by the Cambridge Crystallographic Data Centre.

Crystal data for **2**: $C_{41}H_{30}IrN_4$, CF_3O_3S, 0.5(C_6H_5F), mol wt 968.01, orange, irregular block (0.158 x 0.094 x 0.093), monoclinic, space group $P2_1$, *a*: 14.950(2) Å, *b*: 13.7262(18) Å, *c*: 18.101(2) Å, *β*: 92.045(2)°, *V* = 3712.0(9) Å^3, *Z* = 4, *Z'* = 2, D_{calc}: 1.732 g cm^{-3}, *F*(000): 1916, *T* = 100(2) K, μ = 3.720 mm^{-1}. 34587 measured reflections (2θ = 3−58^o, ω scans 0.3^o), 16725 unique (R_{int} = 0.0782); minimum/maximum transmission factors 0.684/0.862. The final agreement factors were R^1 = 0.0693 (12222 observed reflections, $I > 2\sigma(I)$) and wR^2 = 0.1457; Flack parameter 0.245(16); data/restraints/parameters 16725/1/1004; GOF = 1.059. Largest peak and hole 3.241 (close to iridium atom) and -1.370 e Å^{-3}.

Crystal data for **3**: $C_{35}H_{27}IrN_3O$, CF_3O_3S, mol wt 846.86, yellow, irregular block (0.163 x 0.063 x 0.046), monoclincic, space group $P2_1/c$, *a*: 9.6784(12) Å, *b*: 16.165(2) Å, *c*: 19.539(3) Å, *β*: 99.870(2)°, *V* = 3011.8(7) Å^3, *Z* = 4, *Z'* = 1, D_{calc}: 1.868 g cm^{-3}, *F*(000): 1664, *T* = 100(2) K, μ = 4.570 mm^{-1}. 37919 measured reflections (2θ = 3−58^o, ω scans 0.3^o), 7864 unique (R_{int} = 0.0552); minimum/maximum transmission factors 0.694/0.862. Final agreement factors were R^1 = 0.0288 (5872 observed reflections, $I > 2\sigma(I)$) and wR^2 = 0.0623;

data/restraints/parameters 7864/0/441; GOF = 1.019. Largest peak and hole 1.316 (close to iridium atoms) and -0.980 e Å^{-3}.

Crystal data for **5**: $C_{35}H_{26}IrN_3O$, $2(CH_2Cl_2)$, mol wt 866.64, orange, irregular block (0.224 x 0.173 x 0.160), monoclinic, space group $P2_1/c$, *a*: 12.2654(6) Å, *b*: 15.2776(8) Å, *c*: 17.6216(9) Å, *β*: 98.2780(10)°, *V* = 3267.6(3) Å^3, *Z* = 4, *Z'* = 1, D_{calc}: 1.762 g cm^{-3}, *F*(000): 1704, *T* = 100(2) K, μ = 4.449 mm^{-1}. 33528 measured reflections (2θ = 3−57°, ω scans 0.3°), 7836 unique (R_{int} = 0.0353); minimum/maximum transmission factors 0.694/0.862. Final agreement factors were R^1 = 0.0315 (6675 observed reflections, $I > 2\sigma(I)$) and wR^2 = 0.0782; data/restraints/parameters 7836/0/417; GOF = 1.029. Largest peak and hole 2.132 (close to iridium atoms) and -1.326 e Å^{-3}.

Computational details: All calculations were performed at the DFT level using the B3LYP functional[32] supplemented with the Grimme's dispersion correction D3[33] as implemented in Gaussian09.[34] The Ir atom was described by means of an effective core potential SDD for the inner electrons[35] and its associated double-ζ basis set for the outer ones, complemented with a set of f-polarization functions.[36] The 6-31G** basis set was used for the H, C, N, and O atoms.[37] All minima were verified to have no negative frequencies. The geometries were fully optimized in vacuo and in THF (ε = 7.4257) solvent using the continuum SMD model.[38] We performed TD-DFT calculations at the same level of theory in THF calculating the lowest 50 singlet-singlet excitations at the ground state S_0. It has to be noticed that the singlet-triplet excitations are set to 0 due to the neglect of spin-orbit coupling in the TDDFT calculations as implemented in G09. The UV/vis absorption spectra were obtained by using the GaussSum 3 software.[39] The phosphorescence emission compares well with the 0-0 transition calculated taking into account the zero point energies (zpe) of the geometries of both the optimized S_0 and T_1 states in THF.

Acknowledgements

Financial support from the Spanish MINECO (Projects CTQ2014-52799-P, Red de Excelencia Consolider CTQ2016-81797-REDC), Gobierno de Aragón (E35), FEDER, and the European Social Fund (FSE) is acknowledged.

Keywords: η^1-arene complexes • heteroleptic • iridium • phosphorescent • tridentate ligands •

[1] A. Falceto, E. Carmona, S. Alvarez, *Organometallics* **2014***, 33,* 6660−6668.

[2] S. M. Hubig, S. V. Lindeman, J. K. Kochi, *Coord. Chem. Rev*. **2000**, *200−202*, 831−873.

[3] For example: a) J. Terheijden, G. van Koten, I. C. Vinke, A. L. Spek, *J. Am. Chem. Soc*. **1985**, *107*, 2891−2898; b) J. Forniés, B. Menjón, N. Gómez, M. Tomás, *Organometallics* **1992**, *11*, 1187−1193.

[4] a) R. Rathore, J. Hecht, J. K. Kochi, *J. Am. Chem. Soc*. **1998**, *120*, 13278−13279; b) C. A. Reed, K.-C. Kim, E. S. Stoyanov, D. Stasko, F. S. Tham, L. J. Mueller, P. D. W. Boyd, *J. Am. Chem. Soc*. **2003**, *125*, 1796−1804.

[5] a) L. R. Falvello, J. Forniés, R. Navarro, V. Sicila, M. Tomás, *J. Chem. Soc. Dalton Trans*. **1994**, 3143−3148; b) J. Cámpora, J. A. López, P. Palma, P. Valerga, E. Spillner, E. Carmona, *Angew. Chem. Int. Ed*. **1999**, *38*, 147−151; c) J. Cámpora, E. Gutiérrez-Puebla, J. A. López, A. Monge, P. Palma, D. del Río, E. Carmona, *Angew. Chem. Int. Ed*. **2001**, *40*, 3641−3644; d) S. M. Reid, R. C. Boyle, J. T. Mague, M. J. Fink, *J. Am. Chem. Soc*. **2003**, *125*, 7816−7817; e) S. D. Walker, T. E. Barder, J. R. Martinelli, S. L. Buchwald, *Angew. Chem. Int. Ed*. **2004**, *43*, 1871−1876; f) J. R. Krumper, M. Gerisch, A. Magistrato, U. Rothlisberger, R. G. Bergman, T. D. Tilley, *J. Am. Chem. Soc*. **2004**, *126*, 12492−12502; g) M. Sakamoto, Y. Ohki, K. Tatsumi, *Organometallics*, **2010**, *29*, 1761−1770; h) C. Barthes, C. Lepetit, Y. Canac, C. Duhayon, D. Zargarian, R.Chauvin *Inorg. Chem*. **2013**, *52*, 48−58; i) C. Lepetit, J. Poater, M. E. Alikhani, B. Silvi, Y. Canac, J. Contreras-García, M. Solà, R. Chauvin *Inorg. Chem*. **2015**, *54*, 2960−2969.

[6] a) J. Li, A. C. Grimsdale, *Chem. Soc. Rev*. **2010**, *39*, 2399–2410; b) Y. Tao, Q. Wang, C. Yang, C. Zhong, K. Zhang, J. Qin, D. Ma *Adv. Funct. Mater*. **2010**, *20*, 304–311; c) M. A. Reddy, A. Thomas, G. Mallesham, B. Sridhar, V. J. Rao, K. Bhanuprakash, *Tetrahedron Let*. **2011**, *52*, 6942–6947; d) M. S. Park, J. Y. Lee, *Org. Electron*. **2013**, *14*, 1291–1296; e) G. H. Kim, R. Lampande, M. J. Park, H. W. Bae, J. H. Kong, J. H. Kwon, J. H. Park, Y. W. Park, C. E. Song, *J. Phys. Chem. C* **2014**, *118*, 28757−28763; f) H. Shi, D. Xin, S.-D. Bai, L. Fang, X.-E. Duan, J. Roose, H. Peng, S. Chen, B. Z. Tang, *Org. Electron*. **2016**, *33*, 78–87; g) M. Reig, G. Bubniene, W. Cambarau, V. Jankauskas, V. Getautis, E. Palomares, E. Martínez-Ferrero, D. Velasco, *RSC Adv*., **2016**, *6*, 9247–9253.

[7] For example: a) J. J. Garcia, A. L. Casado, A. Iretskii, H. Adams, P. Maitlis, M. *J. Organomet. Chem*. **1998**, *558*, 189–192; b) A. E. Ashley, A. R. Cowley, J. C. Green, D. R. Johnston, D. J. Watkin, D. L. Kays, *Eur. J. Inorg. Chem.* **2009**, 2547–2552; c) A. J. Blake, W. Lewis, J. McMaster, R. S. Moorhouse, G. J. Moxey, D. L. Kays, *Dalton Trans*. **2011**, *40*, 1641–1645.

[8] a) B. Wucher, M. Moser, S. A. Schumacher, F. Rominger, D. Kunz, *Angew. Chem. Int. Ed*. **2009**, *48*, 4417–4421; b) A. Seyboldt, B. Wucher, S. Hohnstein, K. Eichele, F. Rominger, K. W. Tönroos, D. Kunz, *Organometallics* **2015**, *34*, 2717−2725; c) D. C. Marelius, E. H. Darrow, C. E. Moore, J. A. Golen, A. L. Rheingold, D. B. Grotjahn, *Chem. Eur. J*. **2015**, *21*, 10988–10992; d) A. Seyboldt, B. Wucher, M. Alles, F. Rominger, C. Maichle-Mössmer, D. Kunz, *J. Organomet. Chem*. **2015**, *775*, 202–208; e) E. Jürgens, K. N. Buys, A.-T. Schmidt, S. K. Furfari, M. L. Cole, M. Moser, F. Rominger, D. Kunz, *New J. Chem.,* **2016**, *40*, 9160–9169.

[9] For example: G. T. Plundrich, H. Wadepohl, E. Clot, L. H. Gade, *Chem. Eur. J*. **2016**, *22*, 9283–9292.

[10] For example: a) V. C. Gibson, S. K. Spitzmesser, A. J. P. White, D. J. Williams, *Dalton Trans*. **2003**, 2718–2727; b) A. M. Hollas, W. Gu, N. Bhuvanesh, O. Ozerov, V. *Inorg. Chem*. **2011**, *50*, 3673–3679.

[11] a) C.-L. Ho, Q. Wang, C.-S. Lam, W.-Y. Wong, D. Ma, L. Wang, Z.-Q. Gao, C.-H. Chen, K.-W. Cheah, Z. Lin, *Chem. Asian J*. **2009**, *4*, 89–103; b) S. C. F. Kui, F.-F. Hung, S.-L. Lai, M.-Y. Yuen, C.-C. Kwok, K.-H. Low, S. S.-Y. Chui, C.-M. Che, *Chem. Eur. J*. **2012**, *18*, 96–109; c) C.-L. Ho, L.-C. Chi, W.-Y. Hung, W.-J. Chen, Y.-C. Lin, H. Wu, E. Mondal, G.-J. Zhou, K.-T. Wong, W.-Y. Wong, *J. Mater. Chem*., **2012**, *22*, 215–224; d) M. Tavasli, T. N. Moore, Y. Zheng, M. R. Bryce, M. A. Fox, G. C. Griffiths, V. Jankus, H. A. Al-Attar, A. P. Monkman, *J. Mater. Chem*., **2012**, *22*, 6419–6428; e) J. Li, R. Wang, R. Yang, W. Zhou, X. Wang, *J. Mater. Chem. C*, **2013**, *1*, 4171–4179.

[12] a) R. Zhu, J. Lin, G.-A. Wen, S.-J. Liu, J.-H. Wan, J.-C. Feng, Q.-L. Fan, G.-Y. Zhong, W. Wei, W. Huang, *Chem. Lett*. **2005**, *34*, 1668–1669; b) V. Thamilarasan, A. Jayamani, P. Manisankar, Y.-I. Kim, N. Sengottuvelan, *Inorg. Chim. Acta* **2013**, *408*, 240–245; c) J.-H. Chu, C.-C. Wu, D.-H. Chang, Y.-M. Lee, M.-J. Wu, *Organometallics* **2013**, *32*, 272−282; d) R. Qiu, V. P. Reddy, T. Iwasaki, N.Kambe, *J. Org. Chem*. **2015**, *80*, 367−374.

[13] For example: a) V. K. Rai, M. Nishiura, M. Takimoto, S. Zhao, Y. Liu, Z. Hou, *Inorg. Chem*. **2012**, 51, 822−835; b) T. Yu, Y. Cao, W. Su, C. Zhang, Y. Zhao, D. Fan, M. Huang, K. Yue, S. Z. D. Cheng, *RSC Adv*. **2014**, *4*, 554–562; c) Y. Feng, P. Li, X. Zhuang, K. Ye, T. Peng, Y. Liu,

Y. Wang, *Chem. Commun.* **2015**, *51*, 12544–12547; d) M. Lepeltier, F. Appaix, Y. Y. Liao, F. Dumur, J. Marrot, T. L. Bahers, C. Andraud, C. Monnereau, *Inorg. Chem.* **2016**, *55*, 9586−9595; e) L. Pan, M.-Y. Xu, L.-J. Feng, Q. Chen, Y.-J. He, B.-H. Han, *Polym. Chem*., **2016**, *7*, 2299–2307; f) T. Yu, Z. Xu, W. Su, Y. Zhao, H. Zhang, Y. Bao, *Dalton Trans*. **2016**, *45*, 13491–13502; g) A. Chowdhury, P. Howlader, P. S. Mukherjee, *Chem. Eur. J.* **2016**, *22*, 7468–7478; h) T. Yu, F. Yang, X. Chen, W. Su, Y. Zhao, H. Zhang, J. Li, *New J. Chem.* **2017**, *41*, 2046–2054; i) F. K.-W. Kong, M.-C. Tang, Y.-C. Wong, M. Ng, M.-Y. Chan, V. W.-W. Yam, *J. Am. Chem. Soc*. **2017**, *139*, 6351−6362.

[14] a) J. A. G. Williams, A. J. Wilkinson, V. L. Whittle, *Dalton Trans.* **2008**, 2081–2099; b) C. Ulbricht, B. Beyer, C. Friebe, A. Winter, U. S. Schubert, *Adv. Mater*. **2009**, *21*, 4418–4441; c) Y. You, S. Y. Park, *Dalton Trans.* **2009**, 1267–1282; d) J. A. G. Williams, *Chem. Soc. Rev*. **2009**, *38*, 1783–1801; e) Y. Chi, P.-T. Chou, *Chem. Soc. Rev*. **2010**, *39*, 638–655; f) K. P. S. Zanoni, R. L. Coppo, R. C. Amaral, N. Y. M. Iha, *Dalton Trans*. **2015**, *44*, 14559–14573; g) I. Omae, *Coord. Chem. Rev*. **2016**, *310*, 154−169; h) Y. Chi, T.-K. Chang, P. Ganesan, P. Rajakannu, *Coord. Chem. Rev*. **2017**, *346*, 91−100.

[15] a) R. D. Costa, E. Ortí, H. J. Bolink, F. Monti, G. Accorsi, N. Armaroli, *Angew. Chem. Int. Ed*. **2012**, *51*, 8178–8211; b) T. Hu, L. He, L. Duan, Y. Qiu, *J. Mater. Chem*. **2012**, *22*, 4206–4215; c) K. J. Suhr, L. D. Bastatas, Y. Shen, L. A. Mitchell, G. A. Frazier, D. W. Taylor, J. D. Slinker, B. J. Holliday, *Dalton Trans*. **2016**, *45*, 17807–17823.

[16] a) D. Ma, C. Zhang, Y. Qiu, L. Duan, *Org. Electron*. **2016**, *39*, 16–24; b) F. Zhang, W. Li, D. Wei, X. Dong, S. Li, Z. Li, F. Zhang, X. Wei, B. Wei, G. Cao, B. Zhai, *Inorg. Chim. Acta* **2016**, *453*, 115–121.

[17] For example. a) P. Brulatti, R. J. Gildea, J. A. K. Howard, V. Fattori, M. Cocchi, J. A. G. Williams, *Inorg. Chem*. **2012**, *51*, 3813−3826; b) R. G. Alabau, B. Eguillor, J. Esler, M. A. Esteruelas, M. Oliván, E. Oñate, J.-Y. Tsai, C. Xia, *Organometallics* **2014**, *33*, 5582−5596; c) T. Duan, T.-K. Chang, Y. Chi, J.-Y. Wang, Z.-N. Chen, W.-Y. Hung, C.-H. Chen, G.-H. Lee, *Dalton Trans*. **2015**, *44*, 14613−14624; d) Q.-L. Xu, X. Liang, L. Jiang, Y. Zhao, Y.-X. Zheng, *Dalton Trans*. **2016**, *45*, 7366–7372; e) B. Umamahesh, N. S. Karthikeyan, K. I. Sathiyanarayanan, J. M. Malicka, M. Cocchi, *J. Mater. Chem. C* **2016**, *4*, 10053−10060; f) H. Benjamin, J. Liang, Y. Liu, Y. Geng, X. Liu, D. Zhu, A. S. Batsanov, M. R. Bryce, *Organometallics* **2017**, *36*, 1810−1821; g) H.-H. Kuo, Y.-T. Chen, L. R. Devereux, C.-C. Wu, M. A. Fox, C.-Y. Kuei, Y. Chi, G.-H. Lee, *Adv. Mater.* **2017**, *29*, 1702464.

[18] a) X. Xu, X. Yang, Y. Wu, G. Zhou, C. Wu, W.-Y. Wong, *Chem. Asian J*. **2015**, *10*, 252−262; b) J.-L. Liao, Y. Chi, Z.-T. Sie, C.-H. Ku, C.-H. Chang, M. A. Fox, P. J. Low, M.-R. Tseng, G.-H. Lee, *Inorg. Chem*. **2015**, *54*, 10811−10821; c) S. Yi, J.-H. Kim, Y.-J. Cho, J. Lee, T.-S. Choi, D. W. Cho, C. Pac, W.-S. Han, H.-J. Son, S. O. Kang, *Inorg. Chem*. **2016**, *55*, 3324−3331; d) J. C. Axtell, K. O. Kirlikovali, P. I. Djurovich, D. Jung, V. T. Nguyen, B. Munekiyo, A. T. Royappa, A. L. Rheingold, A. M. Spokoyny, *J. Am. Chem. Soc*. **2016**, *138*, 15758−15765; e) M. A. Esteruelas, E. Oñate, A. U. Palacios, *Organometallics* **2017**, *36*, 1743−1755.

[19] 4 and 5 are the electrons donated by the ligands, whereas t and t' indicate the denticity of the ligands (tridentate). See Ref. [18e].

[20] a) A. J. Wilkinson, A. E. Goeta, C. E. Foster, J. A. G. Williams, *Inorg. Chem*. **2004**, *43*, 6513−6515; b) A. J. Wilkinson, H. Puschmann, J. A. K. Howard, C. E. Foster, J. A. G. Williams, *Inorg. Chem*. **2006**, *45*, 8685−8699; c) J.-L. Chen, Y.-H. Wu, L.-H. He, H.-R. Wen, J. Liao, R. Hong, *Organometallics* **2010**, *29*, 2882–2891; d) Y. Koga, M. Kamo, Y. Yamada, T. Matsumoto, K. Matsubara, *Eur. J. Inorg. Chem*. **2011**, 2869–2878; e) B. Tong, H.-Y. Ku, I.-J. Chen, Y. Chi, H.-C. Kao, C.-C. Yeh, C.-H. Chang, S.-H. Liu, G.-H. Lee, P.-T. Chou, *J. Mater. Chem. C* **2015**, *3*, 3460–3471; f) C.-Y. Kuei, W.-L. Tsai, B. Tong, M. Jiao, W.-K. Lee, Y. Chi, C.-C. Wu, S.-H. Liu, G.-H. Lee, P.-T. Chou, *Adv. Mater*. **2016**, *28*, 2795–2800; g) C.-Y. Kuei, S.-H. Liu, P.-T. Chou, G.-H. Lee, Y. Chi, *Dalton Trans*. **2016**, *45*, 15364–15373; h) J. Lin, N.-Y. Chau, J.-L. Liao, W. Y. Wong, C.-Y. Lu, Z.-T. Sie, C.-H. Chang, M. A. Fox, P. J. Low, G.-H. Lee, Y. Chi, *Organometallics* **2016**, *35*, 1813−1824.

[21] K. H. Lee, H. J. Kang, H. M. Kim, J. H. Seo, Y. K. Kim, S. S. Yoon, *J. Nanosci. Nanotechnol*. **2011**, *11*, 1499–1502.

[22] T. Chen, Q. Huang, Y. Luo, Y. Hu, W. Lu, *Tetrahedron Let*. **2013**, *54*, 1401–1404.

[23] B. Eguillor, M. A. Esteruelas, V. Lezáun, M. Oliván, E. Oñate, *Chem. Eur. J.* **2017**, *23*, 1526–1530.

[24] M. A. Esteruelas, A. M. López, M. Oliván, *Chem. Rev*. **2016**, *116*, 8770−8847.

[25] a) M. Brookhart, M. L. H. Green, *J. Organomet. Chem*. **1983**, *250*, 395–408; b) M. Brookhart, M. L. H. Green, G. Parkin, *Proc. Natl. Acad. Sci. USA* **2007**, *104*, 6908−6914; c) I. Omae, *J. Organomet. Chem*. **2011**, *696*, 1128–1145.

[26] D. Braga, F. Grepioni, K. Biradha, G. R. Desiraju, *J. Chem. Soc. Dalton Trans.* **1996**, 3925–3930.

[27] T. J. Geldbach, D. Drago, P. S. Pregosin, *J. Organomet. Chem*. **2002**, *643-644*, 214–222.

[28] See for example Refs [17a], [18e], [20], and: a) S. Lamansky, P. Djurovich, D. Murphy, F. Abdel-Razzaq, R. Kwong, I. Tsyba, M. Bortz, B. Mui, R. Bau, M. E. Thompson, *Inorg. Chem*. **2001**, *40*, 1704−1711; b) J. Li, P. I. Djurovich, B. D. Alleyne, M. Yousufuddin, N. N. Ho, J. C. Thomas, J. C. Peters, R. Bau, M. Thompson, E. *Inorg. Chem***. 2005**, *44*, 1713−1727; c) T.-Y. Li, X. Liang, L. Zhou, C. Wu, S. Zhang, X. Liu, G.-Z. Lu, L.-S. Xue, Y.-X. Zheng, J.-L. Zuo, *Inorg. Chem*. **2015**, *54*, 161−173; d) V. H. Nguyen, R. S. H. Khoo, J. H. K. Yip, *Inorg. Chem*. **2015**, *54*, 2264−2277.

[29] K. P. S. Zanoni, B. K. Kariyazaki, A. Ito, M. K. Brennaman, T. J. Meyer, N. Y. M. Iha, *Inorg. Chem*. **2014**, *53*, 4089−4099.

[30] R. H. Blessing, *Acta Crystallogr., Sect. A: Found. Crystallogr.* **1995**, *51*, 33−38. *SADABS: Area-detector absorption correction*; Bruker-AXS, Madison, WI, 1996.

[31] SHELXL-2016/6. Sheldrick, G. M. *Acta Cryst. Sect. A: Found. Crystallogr*. **2008**, *64*, 112−122.

[32] a) C. Lee, W. Yang, R. G. Parr, *Phys. Rev. B: Condens. Matter Mater. Phys.* **1988**, *37*, 785−789; b) A. D. *J.* Becke, *Chem. Phys.* **1993**, *98*, 5648−5652; c) P. J. Stephens, F. J. Devlin, C. F. Chabalowski, M. J. Frisch, *J. Phys. Chem*. **1994**, *98*, 11623−11627.

[33] S. Grimme, J. Antony, S. Ehrlich, H. Krieg, *J. Chem. Phys*. **2010**, *132*, 154104.

[34] M. J. Frisch, G. W. Trucks, H. B. Schlegel, G. E. Scuseria, M. A. Robb, J. R. Cheeseman, G. Scalmani, V. Barone, B. Mennucci, G. A. Petersson, H. Nakatsuji, M. Caricato, X. Li, H. P. Hratchian, A. F. Izmaylov, J. Bloino, G. Zheng, J. L. Sonnenberg, M. Hada, M. Ehara, K. Toyota, R. Fukuda, J. Hasegawa, M. Ishida, T. Nakajima, Y. Honda, O. Kitao, H. Nakai, T. Vreven, J. A. Montgomery, Jr., J. E. Peralta, F. Ogliaro, M. Bearpark, J. J. Heyd, E. Brothers, K. N. Kudin, V. N. Staroverov, T. Keith, R. Kobayashi, J. Normand, K. Raghavachari, A. Rendell, J. C. Burant, S. S. Iyengar, J. Tomasi, M. Cossi, N. Rega, J. M. Millam, M. Klene, J. E. Knox, J. B. Cross, V. Bakken, C. Adamo, J. Jaramillo, R. Gomperts, R. E. Stratmann, O. Yazyev, A. J. Austin, R. Cammi, C. Pomelli, J. W. Ochterski, R. L. Martin, K. Morokuma, V. G. Zakrzewski, G. A. Voth, P. Salvador, J. J. Dannenberg, S. Dapprich, A. D. Daniels, O. Farkas, J. B. Foresman, J. V. Ortiz, J. Cioslowski, D. J. Fox, *Gaussian 09, Revision D.01*; Gaussian, Inc., Wallingford, CT, 2013.

[35] D. Andrae, U. M. Haeussermann, M. Dolg, H. Stoll, Preuss, H. *Theor. Chim. Acta* **1990**, *77*, 123−141.

[36] A. W. Ehlers, M. Bohme, S. Dapprich, A. Gobbi, A. Hollwarth, V. Jonas, K. F. Kohler, R. Stegmann, A. Veldkamp, G. Frenking, *Chem. Phys. Lett*. **1993**, *208*, 111−114.

[37] a) W. J. Hehre, R. Ditchfield, J. A. Pople, *J. Chem. Phys*. **1972**, *56*, 2257−2261. b) M. M. Francl, W. J. Pietro, W. J. Hehre, J. S. Binkley, M. S. Gordon, D. J. DeFrees, J. A. Pople, *J. Chem. Phys*. **1982**, *77*, 3654−3665.

[38] A. V. Marenich, C. J. Cramer, D. G. Truhlar, *J. Phys. Chem. B* **2009**, *113*, 6378−6396.
[39] N. M. O'Boyle, A. L. Tenderholt, K. M. Langner, *J. Comput. Chem.* **2008**, *29*, 839−845.

Entry for the Table of

FULL PAPER

Molecular phosphorescent heteroleptic bis-tridentate iridium(III) complexes with a six-membered heterometallaring in their structure have been prepared via η^1-arene intermediates. They are green emitters, which display short lifetimes in the range 1−10 μs and high quantum yields (0.73 - 0.87) in the solid state

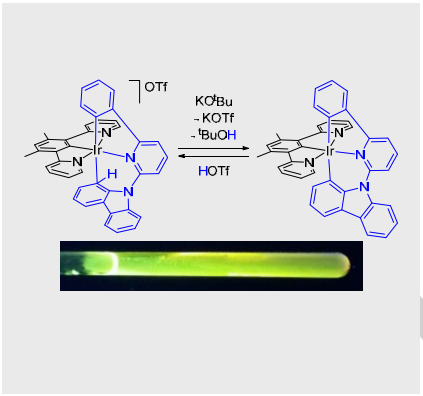

Miguel A. Esteruelas, Daniel Gómez-Bautista, Ana M. López, Enrique Oñate, Jui-Yi Tsai, and Chuanjun Xia*

Page No. – Page No.

η^1-Arene Complexes as Intermediates in the Preparation of Molecular Phosphorescent Iridium(III) Complexes